Cost Estimation of the Sustainable Production of MIL-100(Fe) at Industrial Scale from two upscaled synthesis routes

Maria Inês Severino,[a,b] Cátia Freitas,[a] Vanessa Pimenta,[b] Farid Nouar,[b] Moisés L. Pinto*,[a] Christian Serre*[b]*

[a]*CERENA, Departamento de Engenharia Química, Instituto Superior Técnico, Universidade de Lisboa, 1049-001 Lisboa, Portugal*

[b]*Institut des Matériaux Poreux de Paris, ESPCI Paris, Ecole Normale Supérieure, CNRS, PSL University, 75005 Paris, France*

Email : moises.pinto@tecnico.ulisboa.pt; farid.nouar@espci.psl.eu; christian.serre@espci.psl.eu

Abstract.

Understanding the impact of MOF synthesis conditions on the production cost is vital in order to have a competitive product in a view of industrial applications. Here, considering the benchmark mesoporous iron(III) trimesate MIL-100(Fe) as a prototypical example, we show that the production cost can reach <30 $/kg if a careful selection of the synthetic route is made. Two routes were considered in the analysis, using sulfate and nitrate as iron sources. A new optimized synthesis protocol in a laboratory pilot-scale reactor of 5 liters based on iron sulfate was developed using optimized sustainable ambient pressure conditions, leading to larger particles and a higher STY. Based on reliable pilot-scale data and established chemical engineering estimation methods, this leads to a significantly low production cost of high quality MIL-100(Fe) achieving a potential competitive product.

Graphical abstract:
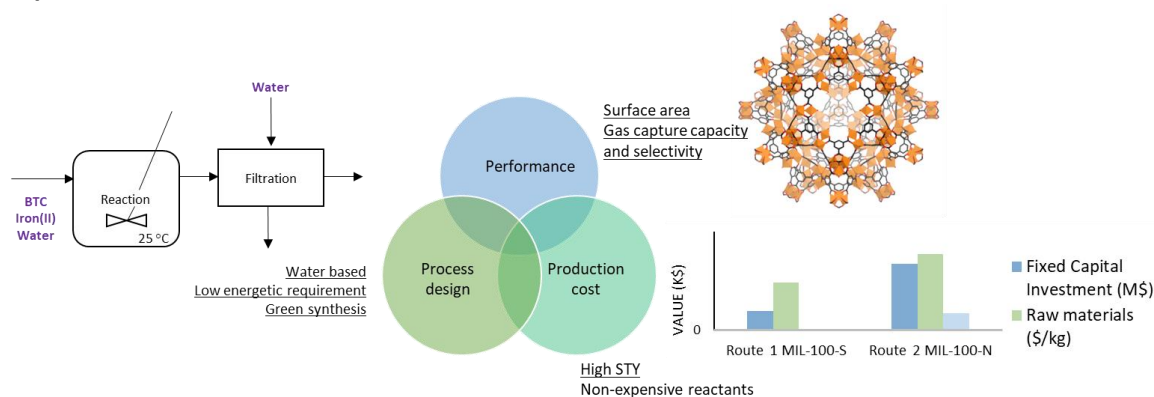
Highlights:

- MIL-100(Fe) can be synthesized in water without any toxic products being required
- High quality high STY sub-micronic particles are obtained in a pilot-scale 5 L reactor
- A benchmark Metal-Organic Framework can be obtained with low industrial production costs

Keywords. Metal-Organic Frameworks, MIL-100(Fe), Scale-up, Green synthesis, Production cost, Industrialization

1. Introduction

Metal-Organic Frameworks (MOFs) are crystalline porous materials whose discovery has been initiated at the end of the 90's[1]. These solids are attractive for a large range of potential applications such as gas storage/separation, sensing, heterogeneous catalysis, energy devices and biomedical applications, among others due to their high porosity, unprecedented chemical and structural versatility.[2] Their interest in real applications has also been increasing recently due to the scale-up of a few benchmark MOFs under green, sustainable and potentially economically viable conditions.

This can be achieved by considering the green chemistry guidelines[3]–[6] which are of particular importance when developing a scalable process.[7] The replacement of the solvent or the decrease of the volume used is one of the main considerations when developing a green process, especially in the case of MOF synthesis, where toxic solvents have been widely used. A first attempt was carried out using cyrene (or dihydrolevoglucosenone) instead of the toxic commonly used *dimethylformamide or* DMF.[8] However, the use of cyrene implies an extra cost due to required effluent treatment or recycling. The use of water or other less-toxic solvents is highly preferable, and there are currently many examples of water-based MOF synthesis in ambient pressure conditions, such as for instance those of the MIL's family : MIL-100(Fe)[9], MIL-101(Cr), MIL-91(Ti, Al),[10], [11], MIL-160(Al)[12], MIL-53(Al)-X's, MIL-53, MIL-53(Al)-NO_2 or -NH_2[13]. Furthermore, other industrially relevant aluminum based MOFs of interest for gas separation or heat reallocation, such as CAU-10(Al) or MOF-303, have also been synthesized using greener protocols at larger scale.[27], [14] The Zr fumarate MOF-801(Zr), of interest for water harvesting, was also obtained in a 5 L pilot-scale using a modulator with a good yield and high

quality[15]; note that the addition of modulators must be considered carefully since it can increase the complexity of the synthesis and possibly the number of synthesis steps (i.e., washing, filtration, etc) as well as promoting structural defects in some cases. The use of alcohols, such as isopropanol, is also an acceptable alternative for instance for the ambient pressure synthesis of MIL-127(Fe)[16], or the synthesis of the new benchmark MOF for CO_2 capture, CALF-20, made in a water/methanol mixture with a very high STY.[17]

At industrial scale, lowering as much as possible the safety and health impacts is essential for the workers, but at the same time the cost is reduced by decreasing the energy requirements or/and by requiring less expensive equipment (e.g., built form noncorrosive resistant materials or ambient pressure equipment). Therefore, ambient pressure, low temperature synthesis associated with the use of non-toxic safe conditions, are beneficial as it is simpler to scale. This requires however a synthesis optimization that carefully selects not only the solvent and relevant synthesis conditions of pressure and temperature but the chemical precursors, such as the metal source or the linker, which should be non-corrosive, non-toxic and abundant. For instance, one shall avoid the use of corrosive counter ions, and thereby carbonates, sulfates and oxides are preferred instead chlorides.[7] In addition, the use of sustainable linkers can result in a lower price, minimal environmental impact and lower toxicity, as well as, having a higher water solubility. This was demonstrated by some of us in the case of the benchmark microporous MIL-160(Al) MOF, of interest for heat reallocation and gas separation, whereas the production cost at industrial scale was estimated to be < 10 \$/kg, at a condition that its constitutive bio-derived linker, 2,5-furandicarboxylic acid, is to be utilized at very

large scale for the production of bioplastics.[18]

Despite these promising studies on the improvement of the production greenness, MOFs are still mainly scaled-up either by startups such as Framergy, MOFtechnologies, MOFapps, Promethean Particles, Numat, NovoMOFs, ProfMOF, Immaterial etc[19] or by large chemical companies such as BASF,[20] however, at the recent exception of CALF-20, still limited amounts envisioned for research and development purposes or for a particular application in lower scale (<ton).[21] As a result the prices are still either unknown or high when available. Nevertheless, these prices are not representative of the real production cost which will depend not only on the final purity required, on the type of process to be considered, raw materials price for bulk production but also on the scale of production. However, the price can be reduced when the raw materials, e.g., the linker are used on other large scale processes, for instance ones that are used in the pharmaceutical industries, plastics production, etc.. Therefore, depending on the parameters considered, the final production cost is much lower than the cost initially estimated in laboratory scale.

A few studies have already explored the production cost of MOFs at multi ton scale. DeSantis et al. explored different synthesis approaches LAG, liquid-assisted grinding, and aqueous synthesis, and estimated that the cost of MOFs can be brought down to less than 10 $/kg for a 2.5 ton/year production[22]. UiO-66(Zr)-NH$_2$ was also recently studied by Luo et al.[23]. In this study, the solvothermal and ambient pressure aqueous-based synthesis were compared in terms of industrial potential. It was clear that with the same production base, the solvothermal synthesis led to higher costs, with a production cost about 3 times higher than the aqueous-based synthesis – 44 $/kg compared with 15 $/kg. This proves the importance of the choice of

production process and its optimization on the estimated production cost. However, this estimation was based on a hypothetical process. Before production cost calculation estimation are assessed, it is important to understand the process scalability using pilot-scale processes. This allows to bridge the laboratory scale where only few mg or g are produced with the industrial scale, where tonnage of the material is produced, confirming the scalability, and optimizing further the process at the 100 g or kg level. This has been done, but not extensively, for several benchmark MOFs, as ZIF-8 producing 6 kg per day in a continuous flow,[24] or for UiO-66(Zr) and its functionalized derivatives UiO-66(Zr)-NH$_2$ and its -COOH form in a solvothermal system giving 647 g in 8 L,[25] or even CAU-10(Al) with 6 kg produced in a 10 L in a 10 hour reflux synthesis.[26], [27]

More recently, an important breakthrough in MOFs was reported with the announcement of the tonnage production of the microporous Zn triazolate-oxalate CALF-20. This MOF, initially reported by Shimizu et al., is currently being produced by BASF in partnership with Svante at multi-hundred ton scale, and the production cost is expected to reach <30 $/kg for the capture of CO$_2$ in cement fabrication.[18], [28], [29] With this recent announcement, it was seen that coupling the high performance potential with the optimization of the production process is essential to achieve scalable production. Furthermore, the estimation of the production cost of some of these materials can help potentiate their consideration in industrial applications.

Some of us have recently proposed for the first time such a comprehensive cost assessment methodology for the prototypical MOF, MIL-160(Al) based on its production in a 30 L pilot-scale reactor.[18] Here, we report a similar approach, based on a newly optimized synthesis protocol, for the benchmark MIL-100(Fe), to estimate its production cost at the

kton scale.[22], [23]

MIL-100(Fe) or $Fe_3O(OH)(C_6H_3(CO_2)_3)_2 \cdot (H_2O)_2 \cdot nH_2O$ is a benchmark iron(III) tricarboxylate MOF built up from trimers of iron octahedra sharing a common vertex μ_3-O.[30], [31] These trimers are then linked by the benzene-1,3,5-tricarboxylate (BTC) moieties in such a way that leads to the formation of hybrid supertetrahedra. This delimits mesoporous cages of free apertures of 25 and 29 Å, accessible through microporous windows of 5.5 and 8.6 Å (Figure 1). MIL-100 shows a very good chemical and thermal stability, a high porosity and the presence of accessible active sites allowing the coordination of different species. It also possesses a biodegradable character associated with a low *in vivo* toxicity[32], [33]. These unique characteristics make MIL-100(Fe) appealing for a wide range of applications such as biomedicine[34], [35], gas storage/separation,[36]–[38] sensing,[39] catalysis,[40]–[42] and heat reallocation,[43], [44]. More recently, we have shown that this MOF, through its open metal sites, can lead to exceptional properties for the capture of traces of acidic volatile organic compounds in humid environments.[45], [46]

The early methods to synthesize MIL-100(Fe) were based on hydrothermal conditions. The small scale protocol reported initially by Horcajada et al.[30] involved iron metal and fluorine and hydrothermal conditions. A fluorine free hydrothermal synthesis was later reported by Seo et al.[9] leading to a pilot-scale production. Despite the high space-time yield (STY) - 252 kg m^{-3} day^{-1} (STY - kg of MOF per m^3 of reactor per day), the use of pressurized hydro/solvo- thermal conditions is not ideal for scale-up production due to safety concerns and high (equipment, energy) costs.[7] A series of ambient pressure synthesis routes have since then been reported for the preparation of MIL-100(Fe) (see Table 1). Some of us have reported very recently a low temperature

green protocol to produce nanoparticles MIL-100(Fe) with a controlled polydispersity suitable for biomedical applications.[47], [48] High
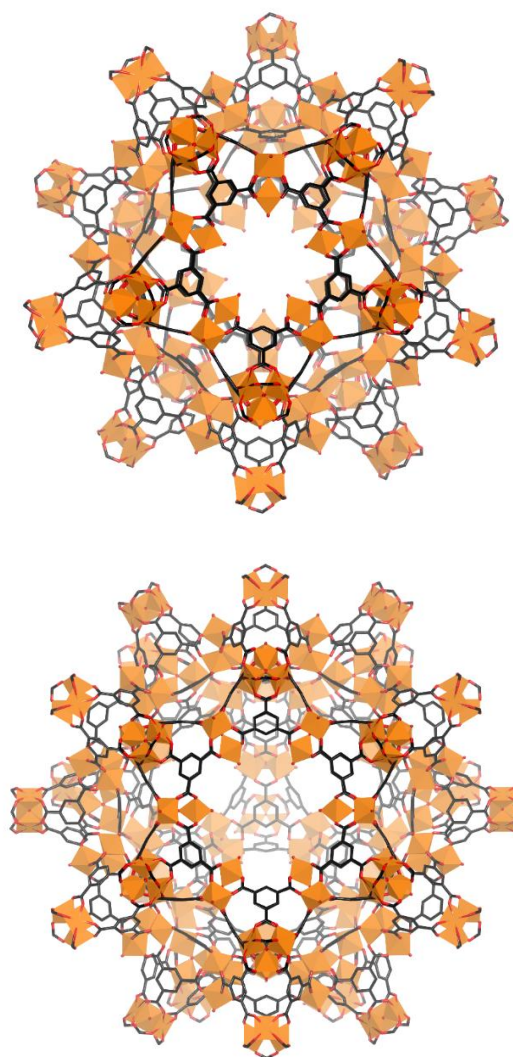

Figure 1 - Schematic view of the MIL-100(Fe) structure with the small S cage (top) and large L cage (bottom) in MIL-100(Fe). Hydrogen atoms are omitted for clarity. Fe octahedra, oxygen and carbon atoms are shown in orange, red, and black,

quality, well faceted 50-60 nm relatively monodisperse nanoparticles with high surface area were obtained, albeit still containing some defects.[49] However the diluted synthesis conditions, associated with a low STY could lead to higher cost productions, although this might not be a major issue for biomedical applications. Guesh et al. proposed in parallel another ambient temperature route with a higher STY (around 30 kg m^{-3} day^{-1}),[50] with

however the use of corrosive chlorides, that would imply a higher production cost due to strict requirements in the equipment construction material as well as increasing safety requirements.[7] On the other hand, the use of sulfate counter anion, that is less corrosive, is highly beneficial for the large scale production of MOFs and has been demonstrated previously for other high valence MOFs such as CAU-10(Al) or UiO-66's[25], [27]. In the case of MIL-100(Fe), this could be strongly beneficial, and has also been reported.[51]–[53] Nevertheless, although greener synthesis conditions are used, the corresponding STY did not exceed 21 kg m^{-3} day^{-1}, reinforcing the need to further optimize the synthesis conditions prior to production cost estimation at the industrial scale.

The production optimization study in the present work was therefore guided by the need to increase the space-time yield while maintaining sustainable conditions, including low energy and materials requirements, suitable for a higher economic viability.[18], [22], [23] A very important parameter when upscaling a given material is to make sure that the upscaled solid keeps a performance similar as the one obtained at laboratory scale. To assess the quality of upscaled MIL-100(Fe), its performance was finally compared to previous ones in the literature for the capture of traces of the polar Volatile Organic compound (VOC) acetic acid.

Two synthesis routes, either relying on iron(III) nitrate or iron(II) sulfate as iron sources,[47], [48] were considered and different parameters optimised in terms of STY and quality (porosity, particle size…) such as temperature, concentration, etc. This led either to monodisperse small size nanoparticles with a low STY for the nitrate route while the sulfate protocol led to much larger particles with a higher STY with a however higher degree of

Table 1 - Ambient pressure synthesis reported in the literature for MIL-100(Fe), precursors and conditions used and characteristics of the material obtained.

Iron source	Solvent	Modulator	T (°C)	Time (hours)	S_{BET} (m^2 g^{-1})	V_{total} (cm^3 g^{-1})	STY (kg m^{-3} day^{-1})	Ref.
Fe^0	Water (DMF)	Benzoquinone/HNO$_3$	RT	12	2482^b	1.0024	-	[59]
Fe(NO$_3$)$_3$	DMSO	HNO$_3$	130	24	1791	0.82	43^c	[60]
Fe(NO$_3$)$_3$	Water (Ethanol)	-	90	18	1212			[61]
Fe(NO$_3$)$_3$	Water	-	60	48	1800		1.6	[47]
FeCl$_3$	Glycol/DMF	-	80	2	2037	1.276	-	[62]
FeCl$_2$	Water (Ethanol)		RT	24				[49]
FeCl$_2$	Water (Ethanol)	NaOH	RT	4	2097	0.81	99^c	[53]
FeSO$_4$/FeCl$_3$	Water	NaOH	RT	24	1180/ 650	1.68	17^c	[50]
FeSO$_4$	Water	NaOH	RT	24	1893	1.024	21^c	[51]
FeSO$_4$	Water (ethanol)	NaOH	RT	15	1542	-	14^c	[52]
		-			2012	-	3^c	

RT room temperature synthesis
^{a}activation at 120 °C
^{b}purified with NH$_4$F
^{c}calculated with 100 % yield and/or considering reaction volume

polydispersity. Their production cost was, therefore, estimated for each metal source based on the optimized conditions and the different elements of the production cost were finally compared and discussed, providing a comprehensive view of the effect of the synthesis route on MOF production cost.

2. Experimental Section
2.1. Materials
All chemicals were purchased from commercial suppliers and used as received without further purifications. 1,3,5-benzene tricarboxylic acid, 98 %, Alfa Aesar. Iron(II) sulfate heptahydrate, 98 %, Sigma-Aldrich, and sodium hydroxide pellets, 98 %, Alfa Aesar, iron(III) nitrate nonahydrate, > 99%, Alfa Aesar.

2.2. Synthesis
a) Nitrate-based Synthesis (MIL-100-N)
Laboratory pilot-scale synthesis
MIL-100(Fe)-N was obtained via ambient pressure synthesis adapted from the conditions referred in the literature.[47], [48] 22.4 g of 1,3,5-benzene tricarboxylic acid (BTC) and 64 g of iron(III) nitrate nonahydrate were added initially to 4 L of deionized water. After 3 hours, the same amount of precursors was added. The mixture was heated to 60°C and stirred for 62 hours in total using a mechanical stirrer. The brown mixture was then filtered to obtain a brown solid which is washed several times with water (2 L) and absolute ethanol (1 L), to remove the unreacted 1,3,5-benzene tricarboxylic acid. The powder was then dried at room temperature (yield = 93% and STY of the reaction ≈ 10 kg m^{-3} day^{-1}).

b) Sulfate-based Synthesis (MIL-100-S)
The sulfate route was optimized in two stages. First the chemical parameters and washing steps were tuned to optimize the synthesis at a few gram scales in terms of crystallinity, purity and STY were determined. Then the scale-up at the laboratory pilot scale using a 5 l reactor was realized.

Small-scale Optimization
Different concentrations were tested, with constant molar ratio, Table 2, and several samples were taken at various synthesis times until 12 hours to monitor the synthesis (crystallinity, purity, yield). The resulting MOF powder was washed directly in the filter with water to remove the unreacted precursors before being dried in a vacuum oven for 15 hours at 150 °C.

This gives for the optimized protocol the following conditions : 8.34 g of iron(II) sulfate heptahydrate and 4.25 g of 1,3,5-benzene tricarboxylic acid (BTC) were added to 40 mL of deionized water and stirred vigorously during 5 minutes at room temperature. 2.42 g of NaOH was dissolved in 40 mL of deionized water and added dropwise to the mixture of iron and BTC. The solution of 1.5 : 1 : 3 Metal : Ligand : NaOH molar ratio was kept under vigorous stirring at room temperature for a total of 12 hours.

The evolution of the synthesis was also followed by the changes in color. After the addition of the NaOH solution to the iron and BTC solution, an initial green precipitate is formed. The solution color slowly turns to yellowish-green then to orangish-brown attributed to the slow oxidation of Fe(II) into Fe(III) required for the formation of iron(III) oxo-trimers of the MIL-100(Fe) structure.

Table 2 - Different reaction conditions tested in the optimization and respective STY of the reaction step for a 12 hours synthesis in a 100 mL flask.

	Ligand (g)	Iron(II) sulfate heptahydrate (g)	Sodium hydroxide (g)	Yield (%)	STY (kg m^{-3} day^{-1})
MIL-100(Fe)-S1	0.85	1.67	0.49	87 %	15
MIL-100(Fe)-S2	2.55	5.01	1.46	67 %	68
MIL-100(Fe)-S3	4.25	8.34	2.42	64 %	95

When the quantity of NaOH was further increased the green solid turned black after just a few minutes which has been previously indicated as a result of the formation of Fe_3O_4 nanorods.[54]

Pilot-scale Room Temperature Synthesis
Using the above-mentioned optimized conditions, the process was scaled-up by performing the reaction in a 5 L pilot-scale glass reactor using mechanical stirring. 315.5 g of iron(II) sulfate heptahydrate and 162.4 g of 1,3,5-benzene tricarboxylic acid were added to 1.5 L of deionized water and stirred vigorously during 5 minutes at room temperature. 92.8 g of NaOH solution was dissolved in 1.5 L deionized water and added dropwise (15 min dropwise addition) to the mixture of iron and BTC. The brown solution was kept under vigorous stirring (900 rpm) at room temperature for 10 hours. The resulting MOF was washed directly in the filter with 6 L of water to remove the side products and unreacted linker before being dried in a vacuum oven for 15 hours at 150 °C (yield = 93 % and STY of the reaction ≈ 120 kg m^{-3} day^{-1}).

2.3. Materials characterization
Routine powder X-ray diffraction (PXRD) data were first recorded using a high-throughput Bruker D8 Advance diffractometer working on transmission mode and equipped with a focusing Göbel mirror producing CuKα radiation (λ = 1.5418 Å) and a LynxEye detector. Transmission infrared spectra were acquired by a Nicolet iS5 FTIR ThermoFisher spectrometer in the range from 4000 to 400 cm^{-1}. Thermogravimetric analysis was performed with a thermogravimetric analyzer Mettler Toledo TGA/DSC 2, STAR System apparatus under oxygen flow at a constant heating rate of 5 °C min^{-1}. A scanning electron microscope (SEM, FEI Magellan) equipped with an energy dispersive X-ray spectrometer (EDX) was used to acquire images as well as to perform elemental analyses on the

synthesized products. The particle size distribution was estimated by using "ImageJ'' software for SEM image processing and analysis. The evaluation of the BET surface area was carried out from Nitrogen sorption isotherms measured at −196 °C in a volumetric automatic apparatus (Micromeritics Tristar), after activation under vacuum at 150 °C for 15 hours.

3. Results and Discussion
3.1. Nitrate-based Synthesis (MIL-100-N)
The increase in concentration of the nitrate-based synthesis, adapted from a previously reported protocol developed by some of us was successfully achieved by the addition of the same amount of precursors after 3 hours of reaction.[47], [48] With this improvement, the STY increased by a factor of 6, i.e. from 1.6 kg m^{-3} day^{-1} to 10 kg m^{-3} day^{-1}, while keeping a monodisperse particle size distribution and an average particle size much lower than 100 nm (Figure S1). The purity of the phase was confirmed by PXRD in comparison with the calculated PXRD pattern, Figure 2 a). The absence of unreacted ligand was also verified by FTIR, Figure S2. In addition, the optimized synthesis showed similar adsorption of nitrogen at 77 K, Figure 2 b), compared to the one reported previously with a BET surface area estimated around 2000 m^2 g^{-1}. The thermal decomposition in oxygen demonstrated a weight loss correspondent to the ligand amount, with a value similar to the theoretical one ($M_{W,ligand}/M_{W,MOF}$ = 37 wt%), Figure S3. This successful laboratory pilot-scale synthesis enabled the production cost estimation of this protocol.

3.2. Sulfate-based Synthesis (MIL-100-S)
a) Small-scale Optimization (MIL-100-S1, S2 and S3)
Starting from the previous green synthesis protocol using iron(II) sulfate heptahydrate as a metal precursor reported by Zhuang et al.[51]
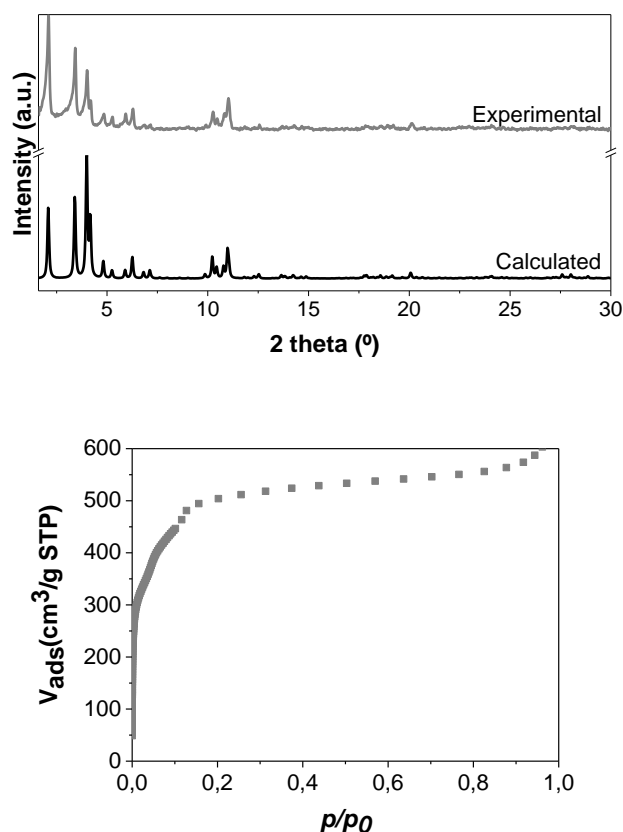
Figure 2 – a) PXRD pattern of MIL-100(Fe)-N synthesized in a 5 L pilot-scale reactor with iron(III) nitrate nonahydrate, in 2Θ range 1.6-30°, compared with the calculated pattern from the literature (CuKα radiation, λ = 1.5418 Å).[30] b) Nitrogen adsorption, at T= -196 ˚C, of MIL-100(Fe)-N in a 5 L pilot-scale reactor with iron(III)nitrate nonahydrate.

We further optimized this protocol to produce samples of MIL-100(Fe)-SX (X=1,2,3) with different concentrations, as summarized in Table 2. Besides the increase in concentration the main differences of the optimized synthesis with regards to the one reported on the literature was the dropwise addition of the sodium hydroxide solution in the metal/ligand aqueous mixture, and the lower synthesis time. The product was formed after 4 hours for the variable concentrations studied, denoted MIL-100(Fe)-S1, MIL-100(Fe)-S2, and MIL-100(Fe)-S3, Figure 3 a). The FTIR confirmed the absence of unreacted linker in all the samples characterized after 4 hours (Figure S4). Furthermore, no crystalline impurities were observed in the diffraction pattern until 60 ˚, Figure S6.

It is of note, that the use of sulfates has been previously reported as being problematic for zirconium-MOFs synthesis. The issue was attributed to the strong interaction between the anions and the framework. For instance, in the case of UiO-66(Zr)-F$_4$ the removal of sulfates required a costly treatment in water at elevated temperature which was only partially achieved (decreasing the SO_4^{2-} ions/Zr_6-cluster ration from 3.6 to 3 after wash).[55] Here, the sulfate contamination was monitored for MIL-100(Fe) through EDX analyses, Table S2. An initial sulfur content of 22 atomic% was observed for the unwashed sample that corresponds to a S/Fe molar ratio of around 0.2. However, as opposite to the UiO-66(Zr)-F$_4$ case, a simple washing step with water at room temperature directly through the filter eliminated the contamination. The same was observed for the sodium, suggesting that the initial sulfate contamination was only related to unreacted precursors. Such a difference is likely to be due to the lower acidic character of iron(III) compared to zirconium(IV) and thus the lower interaction between the iron sites and sulfates.

From the nitrogen isotherms of the samples obtained at different concentrations, Figure 3 b), it is seen that the surface areas, calculated with the BET method, are in fair agreement with values reported in the literature, all reaching values above 1600 m^2 g^{-1}.[56] Nevertheless, these values are still significantly lower than the ones obtained for the nitrate-based synthesis. Such differences of surface area are tentatively assigned to the differences in quality of the samples, previously attributed by Zhuang et al.[51] to agglomerated forms of nanocrystals (kinetic phase of MIL-100(Fe)) and unreacted species (in trace amounts not visible in the FTIR but sufficient to affect adsorption) trapped in the pores. These effects were evidenced by comparing the SEM
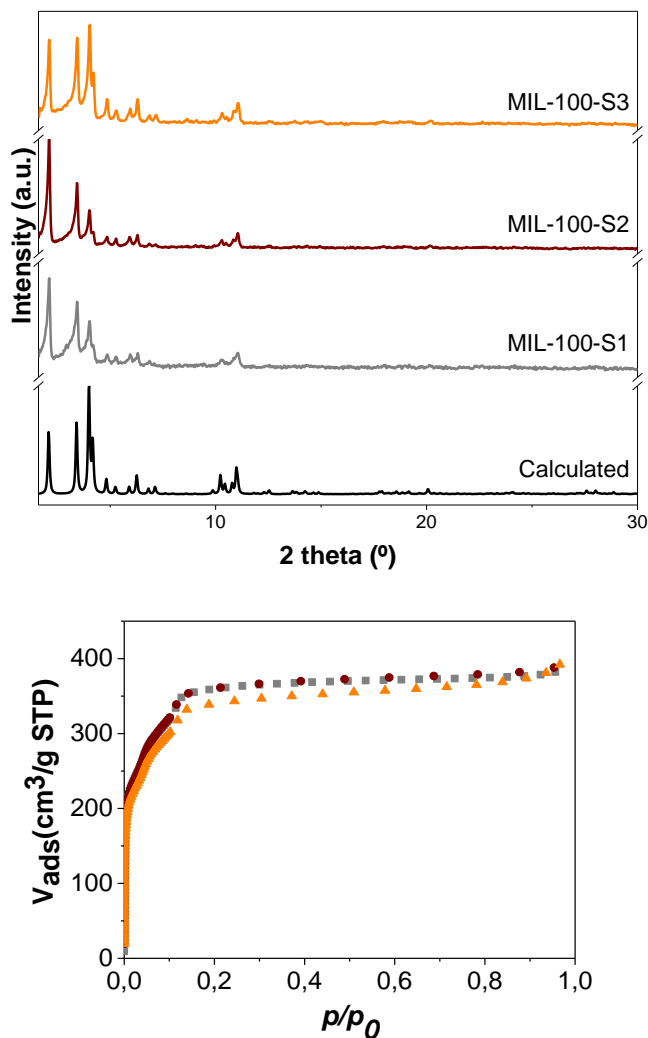
Figure 3 - (a) PXRD patterns of MIL-100(Fe) synthesized in 100 mL round bottom flasks at different concentrations (orange) MIL-100-S3, (Brown) MIL-100-S2 and (grey) MIL-100-S1 in 2Θ range 1.6-30° compared with calculated pattern[30] (black) (CuKα radiation, λ = 1.5418 Å). b) Nitrogen adsorption isotherms, at T=-196 ˚C, of all the different of MIL-100(Fe) samples obtained with different concentrations after 12 hours synthesis (▲) MIL-100-S3, (●) MIL-100-S2 and (■) MIL-100-S1.

confirm that this was the reason behind the decrease in surface area in our work, MIL-100-S3 was left for a 24 hours synthesis. The increase in reaction time led to an increase of surface area reaching around 1850 m^2 g^{-1}, Figure S7[52], [53]. It is of note that, in the recent case of Steenhaut et al.,[53] this value of surface area was obtained after only 15 hours, and, thus, 15 hours instead of 24 hours could be sufficient to obtain high quality MIL-100(Fe). Despite still slightly lower surface areas the value of around 1600 m^2 g^{-1} was considered enough for further pilot-scale trials since it was associated with a high STY, also bearing in mind that the protocol could be further optimized when scaling up this route. Furthermore, one important characteristic of the sulfate route is the formation of larger particles without requiring the use of harsher energy demanding hydrothermal conditions. The particles obtained, although polydisperse whatever the concentration, exhibit a very similar average size value, above 340 nm for the higher concentration (MIL-100(Fe)-S3) and 320 nm for the lower concentration MIL-100(Fe)-S1, Figure 4. The microrods described in the literature were not observed in our case for the 12 hours synthesis. The values of particle size are however smaller than the ones obtained by Tan et al.,[52] that presented a particle size distribution of 1 µm. This can be a result of the shorter reaction time – 12 hours – for MIL-100-S instead of the 24 hours reported before. Nevertheless, the size remains considerably higher than the one reported in other atmospheric pressure synthesis.[47], [54] This is advantageous for most industrial uses in general since smaller particles are harder to handle during the production process and final applications, and can lead to safety issues. Nevertheless, smaller particles could be an advantage for bio-applications, sensing or catalysis, and as such the nitrate optimisation synthesis protocol was also explored, although exhibiting a lower STY.

pictures at different reaction times. With a synthesis time of 4 hours, microrods were observed, probably associated with the formation of a non-porous iron(II) trimesate. In this case, the incomplete reaction led to a lower surface area of 1180 m^2 g^{-1}. Nevertheless, Zhuang et al., showed that the microrods completely disappeared at 24 hours of reaction according to SEM.[51] Therefore, to
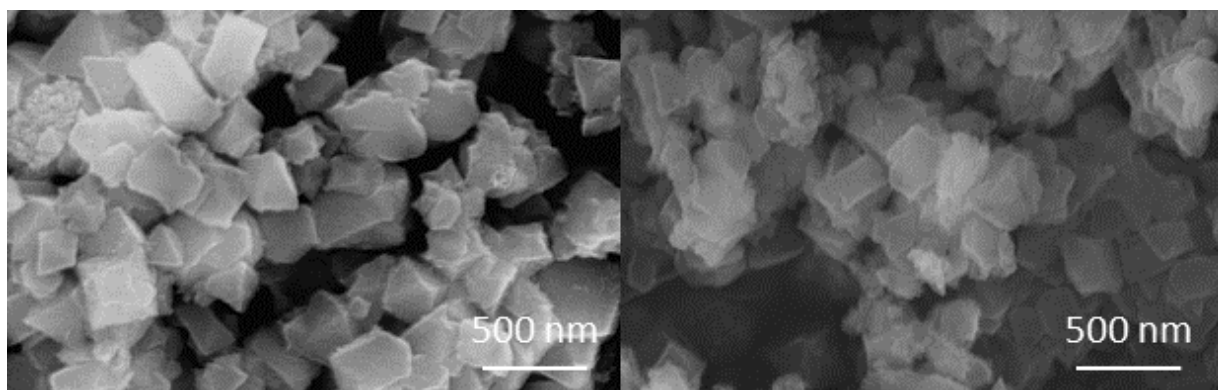
Figure 4 - Comparison of SEM picture of the MOF obtained with synthesis with different concentrations, a) MIL-100(Fe)-S1 and b) MIL-100(Fe)-S3, for 12 hours synthesis.

b) Pilot-laboratory scale synthesis (MIL-100-S-5L)

Given the promises from the optimized small-scale sulfate synthesis, a first upscaling was performed in a larger-scale 5 L pilot reactor. The resulting MOF (MIL-100(Fe)-S-5L) showed a good crystallinity, with its PXRD pattern matching the calculated one and the one of the small-scale sample, Figure 5 a). To assess the quality of the MIL-100(Fe)-S-5L sample, nitrogen porosimetry analysis was carried and showed, Figure 5 b), an improvement in comparison with the small-scale, with around 1900 m^2 g^{-1} being obtained after only 10 hours of reaction. Furthermore, this value is similar to the one of MIL-100-N (Figure 3 b) and is consistent with those of the literature for non HF routes.[47] This improvement is probably due to a more efficient mixing attained with the mechanical stirring in the pilot-scale reactor. Therefore, vigorous stirring was considered essential in this reaction, allowing the improvement of the ligand solubility and to avoid abrupt pH increase upon adding the sodium hydroxide solution. Thus, the scalability of the synthesis was proven to be successful and was the starting point for the techno-economic production cost estimation.

3.3. Production cost estimation

The demonstration of the scalability of the synthesis route, nitrate or sulfate, has been established and paves the way for a preliminary process design. This was done considering all the specifications, the mass
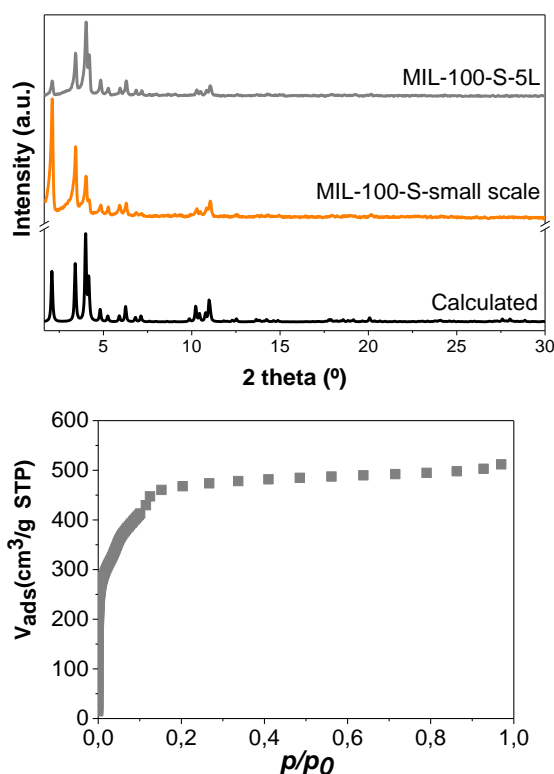

Figure 5 – a) PXRD patterns for MIL-100(Fe) synthesized the 5 L pilot-scale reactor, reactor MIL-100-S-5L (grey) compared with the small scale PXRD (orange), in 2Θ range from 1.6 to 30 ̊, and with the calculated pattern (black), (CuKα radiation, λ = 1.5418 Å), b) Nitrogen adsorption, at -196 ̊C, isotherms of MIL-100(Fe) synthesized in the 5 L pilot-scale reactor (MIL-100-S-5L).

balance and the process design including the most common pieces of equipment, Figure S10. Each equipment was sized based on the mass balance of the process and on known heuristics. The outputs and inputs composition of the main streams are shown in Table 2. The price of each piece of equipment sized or group of equipment based on the mass balance for a 1 kton/year production facility is shown in Table S5. However, the fixed capital investment (FCI) represents not only the capital needed for the installed process equipment but also all the process auxiliaries (e.g., foundations, buildings, structures, piping). Two methods were used to estimate the total FCI: cost factors estimate method and Lang's method, further detailed in Table S5. The higher FCI estimated was obtained with the cost factor method, being this value the one chosen for the production cost estimation.

In the case of the nitrate route, the FCI was much higher than the one obtained for MIL-100(Fe)-S, 20 M\$ against 5 M\$, Figure 6 a). This is a result of the higher volume that is needed in the equipment to achieve the same production capacity, due to the lower concentration and longer synthesis time. Hence, for the production of the same base amount - 1 kton a year, i.e., the lower STY implies higher size of the most relevant pieces of equipment (reactor and filter), Table S5. This production scale was considered to keep within the scales of similar studies previously reported in literature.[18], [22] It is of note that, the size of the pieces of equipment to handle solids is not significantly higher, as it can be seen by the value of the dryer that only increased from 58 k\$ to 77 k\$ Table S5. This is due to the quantity of solid material being handled that is similar in both cases, since it is defined by the production scale considered (i.e., 1 kton).

Therefore, the difference between the two FCI is mostly highly influenced by the reactor's dimension (for MIL-100-N 448 m^3 – 1427 \$/kg and for MIL-100-S 22 m^3 – 248 k\$)), being the optimization of this step crucial for a lower FCI value, as it can be seen in Figure 6 b). It is important to note that the total cost of the equipment, here comprising the reactor, is used to estimate the other parcels of the FCI, i.e., assembly of base equipment, construction expenses, contractor's fee, electric installations, contingency, thermal isolation, by using typical chemical engineering correlations.[57]

Table 3 – Input and output per batch to produce 1 k ton/year.

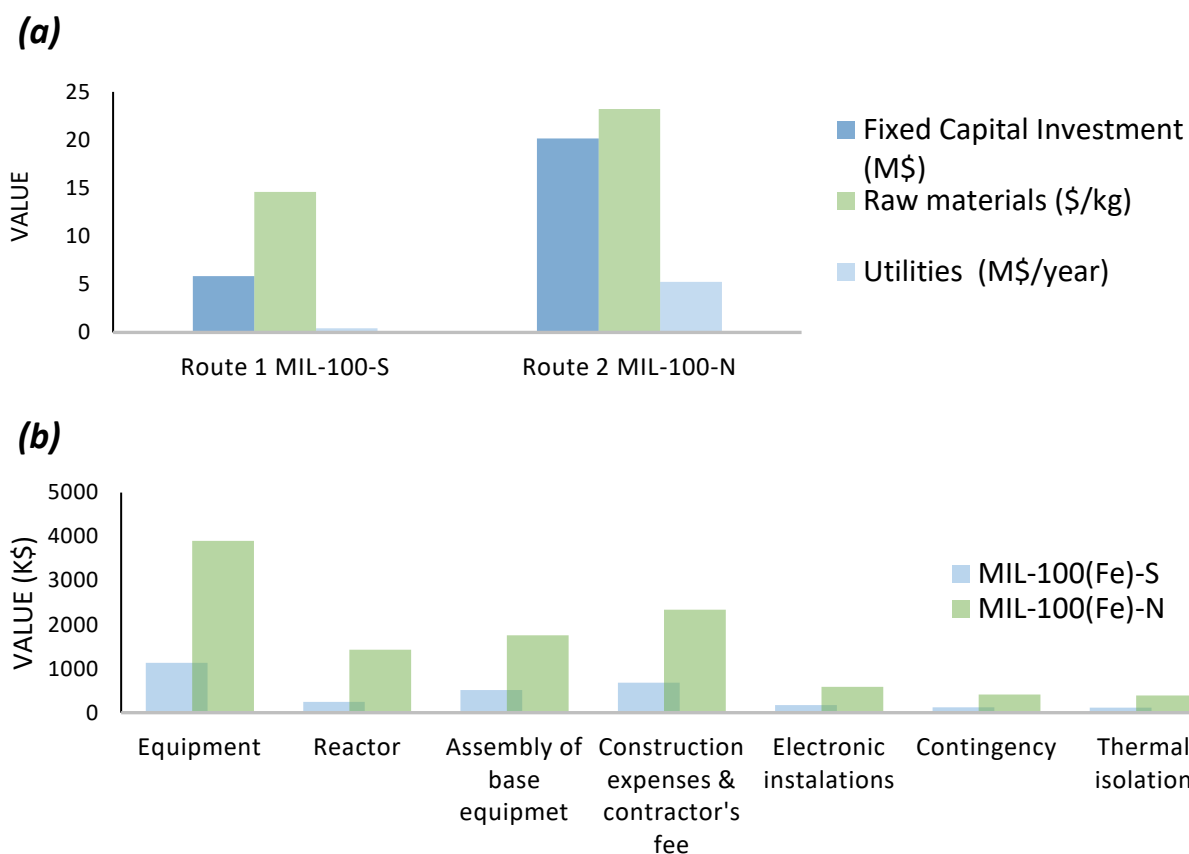| MIL-100-S-5L			
Input		**Output**	
10 hours synthesis			
Water (kg)	16112	MOF (kg)	1244
BTC (kg)	793	Water (kg)	126
Iron(II)	1574		
NaOH (kg)	453	-	-
Energy (MJ/kg)	11	-	-
MIL-100-N-5L			
Input		**Output**	
62 hours synthesis			
Water (kg)	347015	MOF (kg)	7711
BTC (kg)	5134	Water (kg)	779
$Fe(NO_3)_3$	14807		
Energy (MJ/kg)	350	-	-

(a)

(b)

Figure 6 - (a) Impact of the main parcels of the production cost for two different synthetic routes, MIL-100(Fe)-S and MIL-100(Fe)-N and different components that influence the estimated value (b) Fixed capital investment parcels of the sulfate-based synthesis, compared with nitrate base synthesis.

The fixed capital investment (Figure 6 b)) then influenced several values of the cost, i.e., maintenance and repairs, plant overhead costs, operating supplies, insurance, taxes. Other such as the raw materials, utilities, operating labor and supervision, rent and depreciation were determined based on values of the market and respective energy and mass balance.

Since the higher STY leads to lower equipment cost on the counts of lower volume, in the case of the sulfate-based synthesis the production cost is also expected to decrease. Therefore, a lower production cost of only 30 $/kg for 1kTon/year is determined for the sulfate when compared with the nitrate route 58 $/kg. These values already include the capital costs for total investment (not only the FCI) and a project time-span of 10 years.[18] Nonetheless,

the nitrate-based synthesis remains the only one where almost nanometric rather monodisperse size particles can be obtained, which is crucial in high-end applications where the increase in cost could be justified, for instance when it deals with biomedical or sensing applications. The production cost values obtained are also comparable to the one obtained for MIL-160(Al) related to a similar process type. A low value of production cost results, therefore, from the combination of low FCI with lower operational cost, such as low raw materials cost and low energy demand.

Nevertheless, it is clear that the FCI has a much lower impact contributing for the plant overhead costs maintenance and others. FCI influences, thus, less than 20 % of the final value of the production cost, and even if it
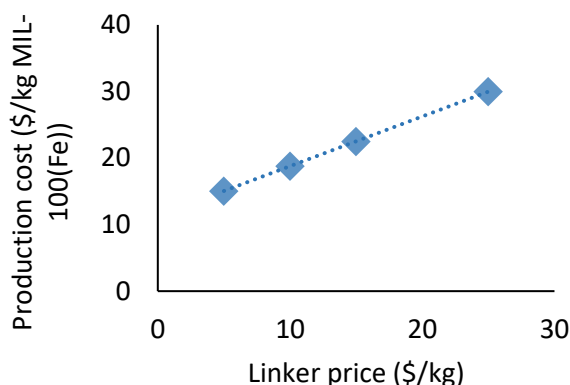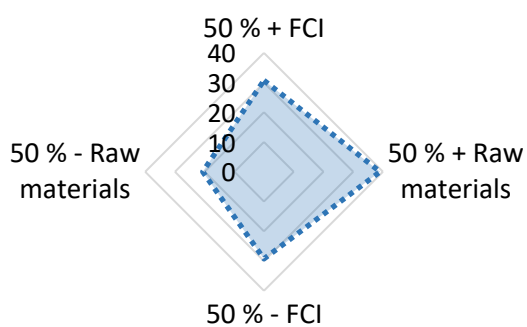
Figure 7 – a) Sensitive analysis of the impact of FCI and Raw materials on the production cost estimated for the MIL-100-S. and b) Production cost of the MIL-100-S compared with different price values for the ligand BTC.

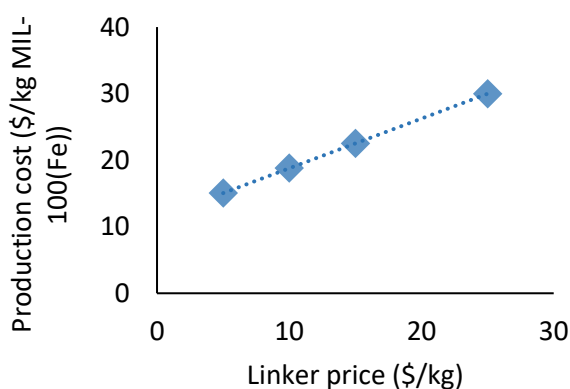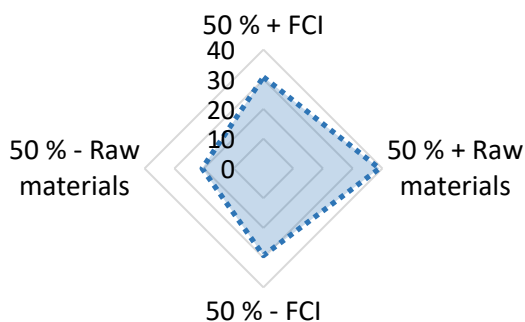varies greatly the impact on the production cost is not affected to the same extent,

Figure 7 a), i.e., if it increases by 50 %, the production cost does not increase by 50 %. Therefore, the most crucial element contributing for this low final value was the low cost considered for the raw materials (or linked elements as the yield), as seen in the literature.[58] If the price of the linker decreases to 10 $/kg (the same price considered for FDCA in the production cost estimation of MIL-160(Al)) the price of MIL-100(Fe) will dramatically decrease down to 19 $/kg, Figure 7 b), and the trend continuous with the further decrease of the linker price.

Our analysis indicates that the production cost value can be lower than 30 $/kg with the room temperature atmospheric pressure method described in this work. This supports the use MIL-100(Fe) for a large diversity of applications, with a value of the production cost being even similar to the first MOF considered recently for the tonnage production, CALF-20.[18], [59] In this work, it is seen by comparing the different parcels that one can target the process optimization with a goal of an even lower production cost value. Additionally, the value of the production cost obtained and the impact of this value on the variations in FCI or raw materials, i.e., sensitive analysis, are also in line with the conclusions from MIL-160(Al) that was obtained with a similar synthetic method, the batch synthesis.[18]

4. Conclusion

The prototypical MIL-100(Fe) possesses an exceptional combination of features, i.e., high porosity, acid/redox open metal sites, green synthesis, chemical stability, and low toxicity that caught the attention of researchers and

industry. These conditions associated with higher STY of 10 kg m^{-3} day^{-1}, obtained after optimization of the synthesis protocol for iron nitrate as the metal source led to a production cost of 58 $/kg while keeping a monodisperse particle size distribution. Another optimized synthesis protocol using less corrosive iron(II) sulfate was also considered and a higher STY, of almost 120 kg m^{-3} day^{-1} was obtained. In this case, we predict that despite the commonly misconception that MOFs are rather expensive materials, MIL-100(Fe) appears to be a prominent MOF candidate to be produced at industrial scale with a production cost of less than 30 $/kg, as a result of the newly optimized ambient pressure green synthesis. The optimization of the synthesis protocols in this work considered all the main constraints in the industrial production, from green conditions, lack of corrosive raw materials, an easy washing method, use of high concentrated solutions in order to have smaller equipment and, consequently lower FCI. In addition, our new protocol does not require any increase in pressure or temperature, requiring less energy and simple pieces of equipment. Nevertheless, the process design followed here a simplistic approach. Several considerations should be analyzed more deeply in the future, such as the recirculation of un-reacted raw materials, that could potentially improve the production cost, or the mandatory effluent treatments which can be more crucial in the case of the nitrate-based synthesis. In sum, this study not only showed the potential of MIL-100(Fe) for industrial production but also allowed the enlightenment of the most important parameters for its economic viability.

Conflicts of interest
There are no conflicts to declare.

Acknowledgements

References

[1] B. F. Hoskins and R. Robson, "Infinite Polymeric Frameworks Consisting of Three Dimensionally Linked Rod-like Segments," *J. Am. Chem. Soc.*, vol. 111, no. 15, pp. 5962–5964, 1989.

[2] P. K. Bharadwaj, P. Feng, *et al.*, "Metal–Organic Frameworks and Their Applications," *Chem. - An Asian J.*, vol. 14, no. 20, pp. 3450–3451, 2019.

[3] F. P. Byrne, S. Jin, *et al.*, "Tools and techniques for solvent selection: green solvent selection guides," *Sustain. Chem. Process.*, vol. 4, no. 1, p. 7, 2016.

[4] D. Prat, A. Wells, *et al.*, "CHEM21 selection guide of classical- and less classical-solvents," *Green Chem.*, vol. 18, no. 1, pp. 288–296, 2015.

[5] P. Isnard, E. Guntrum, *et al.*, "Sanofi's Solvent Selection Guide: A Step Toward More Sustainable Processes," 2013.

[6] "ETH Zurich (2008) EHS assessment tool." [Online]. Available: https://emeritus.setg.ethz.ch/research/downloads/software---tools/ehs-tool.html. [Accessed: 06-Aug-2021].

[7] R. Del Angel, G. Mouchaham, F. Nouar, A. Tissot, C. Serre, *"Robust and Environmentally Friendly MOFs". Metal Organic Frameworks in Biomedical and Environmental Field, P. Horcajada, S. R. Macias*. Springer International Publishing, 2021.

[8] J. Zhang, G. B. White, *et al.*, "Dihydrolevoglucosenone (Cyrene) As a Green Alternative to N,N-Dimethylformamide (DMF) in MOF Synthesis," *ACS Sustain. Chem. Eng.*, vol. 4, no. 12, pp. 7186–7192, 2016.

[9] Y. K. Seo, J. W. Yoon, *et al.*, "Large scale fluorine-free synthesis of hierarchically porous iron(III) trimesate MIL-100(Fe) with a zeolite MTN

topology," *Microporous Mesoporous Mater.*, vol. 157, pp. 137–145, 2012.

[10] V. Benoit, R. S. Pillai, *et al.*, "MIL-91(Ti), a small pore metal-organic framework which fulfils several criteria: An upscaled green synthesis, excellent water stability, high CO2 selectivity and fast CO2 transport," *J. Mater. Chem. A*, no. 4, pp. 1383–1389, 2016.

[11] Z. Kong, Z. Niu, *et al.*, "In situ analysis of the adsorption behaviors of CO2 on the surface of MIL-91(Al)," *New J. Chem.*, vol. 42, no. 20, pp. 16985–16991, 2018.

[12] A. Cadiau, J. S. Lee, *et al.*, "Design of Hydrophilic Metal Organic Framework Water Adsorbents for Heat Reallocation," *Adv. Mater.*, vol. 27, no. 32, pp. 4775–4780, 2015.

[13] M. Sánchez-Sánchez, N. Getachew, *et al.*, "Synthesis of metal-organic frameworks in water at room temperature: Salts as linker sources," *Green Chem.*, vol. 17, no. 3, pp. 1500–1509, 2015.

[14] Z. Zheng, H. L. Nguyen et al., "High-yield, green and scalable methods for producing MOF-303 for water harvesting from desert air", Nat Protoc 2023, 18, 136.

[15] S. Dai, F. Nouar, *et al.*, "One-step versatile room temperature synthesis of metal (IV) carboxylate MOFs To cite this version : HAL Id : hal-03052639 One-step versatile room temperature synthesis of metal (IV) carboxylate MOFs," vol. 60, no. 8, pp. 4282–4288, 2020.

[16] H. Chevreau, A. Permyakova, *et al.*, "Synthesis of the biocompatible and highly stable MIL-127(Fe): From large scale synthesis to particle size control," *CrystEngComm*, vol. 18, no. 22, pp. 4094–4101, 2016.

[17] J. Bin Lin, T. T. T. Nguyen, *et al.*, "A scalable metal-organic framework as a durable physisorbent for carbon dioxide capture," *Science (80-.).*, vol. 374, no. 6574, pp. 1464–1469, 2021.M.

[18] I. Severino, E. Gkaniatsou, *et al.*, "MOFs industrialization: A complete assessment of production costs," *Faraday Discuss.*, vol. 231, pp. 326–341, 2021.

[19] "(a) http://www.framergy.com/ (b)https://www.moftechnologies.com (c) http://www.mofapps.com/ (d) https://prometheanparticles.co.uk/(e) https://profmof.com/ (f) https://immaterial.com/." .

[20] S. C. Josephine Nakhla, "Metal Organic Frameworks (MOFs)." [Online]. Available: https://www.sigmaaldrich.com/US/en/technical-documents/technical-article/materials-science-and-engineering/photovoltaics-and-solar-cells/metal-organic-frameworks. [Accessed: 21-Sep-2021].

[21] U. Ryu, S. Jee, *et al.*, "Recent advances in process engineering and upcoming applications of metal – organic frameworks," *Coord. Chem. Rev.*, vol. 426, p. 213544, 2021.

[22] D. DeSantis, J. A. Mason, *et al.*, "Techno-economic Analysis of Metal−Organic Frameworks for Hydrogen and Natural Gas Storage," *Energy and Fuels*, vol. 31, pp. 2023–2032, 2019.

[23] H. Luo, F. Cheng, *et al.*, "Comparison between conventional solvothermal and aqueous solution-based production of UiO-66-NH2: Life cycle assessment, techno-economic assessment, and implications for CO2capture and storage," *J. Environ. Chem. Eng.*, vol. 9, no. 2, pp. 1–39, 2021.

[24] A. S. Munn, P. W. Dunne, *et al.*, "Large-scale continuous hydrothermal production and activation of ZIF-8," *Chem. Commun.*, vol. 51, no. 64, pp. 12811–12814, 2015.

[25] Y. Khabzina, J. Dhainaut, *et al.*, "Synthesis and Shaping Scale-up Study of Functionalized UiO-66 MOF for Ammonia Air Purification Filters," *Ind. Eng. Chem. Res.*, vol. 57, no. 24, pp. 8200–8208, 2018.

[26] N. S. D. Fröhlich, A. Holz, S. Henninger, D. Lenzen, H. Reinsch,

"WO2017046417 A1 - METHOD FOR PRODUCING METAL-ORGANIC FRAMEWORKS," 2015.

[27] D. Lenzen, P. Bendix, *et al.*, "Scalable Green Synthesis and Full-Scale Test of the Metal–Organic Framework CAU-10-H for Use in Adsorption-Driven Chillers," *Adv. Mater.*, vol. 30, no. 6, pp. 1–6, 2018.

[28] G. Shimizu, R. Vaidhyanathan, *et al.*, "Patent : Metal organic framework, production and use thereof.," no. WO2014138878A1, 2014.

[29] P. Hovington, O. Ghaffari-Nik, *et al.*, "Rapid Cycle Temperature Swing Adsorption Process Using Solid Structured Sorbent for CO2 capture from Cement Flue Gas," *SSRN Electron. J.*, no. March, pp. 1–11, 2021.

[30] P. Horcajada, S. Surblé, *et al.*, "Synthesis and catalytic properties of MIL-100(Fe), an iron(III) carboxylate with large pores," *Chem. Commun.*, vol. 100, no. 27, pp. 2820–2822, 2007.

[31] G. Férey, C. Serre, *et al.*, "A hybrid solid with giant pores prepared by a combination of targeted chemistry, simulation, and powder diffraction," *Angew. Chemie - Int. Ed.*, vol. 43, no. 46, pp. 6296–6301, 2004.

[32] N. Campagnol, R. Romero-vara, *et al.*, "A Hybrid Supercapacitor based on Porous Carbon and the Metal-Organic Framework MIL-100 (Fe)," vol. 100, pp. 1–8, 2014.

[33] T. Baati, L. Njim, *et al.*, "In depth analysis of the in vivo toxicity of nanoparticles of porous iron(iii) metal–organic frameworks," *Chem. Sci.*, vol. 4, no. 4, pp. 1597–1607, 2013.

[34] C. R. Quijia, C. Lima, *et al.*, "Application of MIL-100(Fe) in drug delivery and biomedicine," *J. Drug Deliv. Sci. Technol.*, vol. 61, p. 102217, 2021.

[35] X. Ma, M. Lepoitevin, *et al.*, "Metal-organic frameworks towards bio-medical applications," *Mater. Chem. Front.*, vol. 5, no. 15, pp. 5573–5594, 2021.

[36] M. Latroche, S. Surblé, *et al.*, "Hydrogen Storage in the Giant-Pore Metal–Organic Frameworks MIL-100 and MIL-101," *Angew. Chemie - Int. Ed.*, vol. 118, no. 48, pp. 8407–8411, 2006.

[37] S. Wuttke, P. Bazin, *et al.*, "Discovering the active sites for C3 separation in MIL-100(Fe) by using operando IR spectroscopy," *Chem. - A Eur. J.*, vol. 18, no. 38, pp. 11959–11967, 2012.

[38] J. W. Yoon, Y. K. Seo, *et al.*, "Controlled reducibility of a metal-organic framework with coordinatively unsaturated sites for preferential gas sorption," *Angew. Chemie - Int. Ed.*, vol. 49, no. 34, pp. 5949–5952, 2010.

[39] J. H. Fu, Z. Zhong, *et al.*, "SERS-Active MIL-100(Fe) Sensory Array for Ultrasensitive and Multiplex Detection of VOCs," *Angew. Chemie - Int. Ed.*, vol. 59, no. 46, pp. 20489–20498, 2020.

[40] M. Giménez-Marqués, A. Santiago-Portillo, *et al.*, "Exploring the catalytic performance of a series of bimetallic MIL- 100(Fe, Ni) MOFs," *J. Mater. Chem. A*, vol. 7, no. 35, pp. 20285–20292, 2019.

[41] N. M. Mahmoodi, J. Abdi, *et al.*, "Metal-organic framework (MIL-100 (Fe)): Synthesis, detailed photocatalytic dye degradation ability in colored textile wastewater and recycling," *Mater. Res. Bull.*, vol. 100, pp. 357–366, 2018.

[42] J. N. Hall and P. Bollini, "Metal-Organic Framework MIL-100 Catalyzed Acetalization of Benzaldehyde with Methanol: Lewis or Brønsted Acid Catalysis?," *ACS Catal.*, vol. 10, no. 6, pp. 3750–3763, 2020.

[43] P. Hou, K. Zu, *et al.*, "A novel metal-organic frameworks based humidity pump for indoor moisture control," *Build. Environ.*, vol. 187, p. 107396, 2021.

[44] F. Jeremias, A. Khutia, *et al.*, "MIL-100(Al, Fe) as water adsorbents for heat transformation purposes - A promising application," *J. Mater. Chem.*, vol. 22, no. 20, pp. 10148–10151, 2012.

[45] M.I. Severino Neves, A. Al Mohtar et

al. "[MOFs with Open Metal(III) Sites for the Environmental Capture of Polar Volatile Organic Compounds." Angew. Chem. Int. Ed. 2022, e202211583

[46]   M.I. Severino Neves et al., WO 2023/104665 A1 - "Metal-Organic Frameworks for the selective capture of volatile organic compounds comprising carboxylic acid functional groups."

[47]   M. Panchal, Monik; Nouar, Farid; Serre, Christian; Benzaqui, Marvin; Sene, Saad; Steunou, Nathalie; Gimenez Marqués, "US20210277042A1 - Low temperature process for the synthesis of MOF carboxylate nanoparticles," 2017.

[48]   S. Cui, M. Qin, *et al.*, "Metal-Organic Frameworks as advanced moisture sorbents for energy-efficient high temperature cooling," *Sci. Rep.*, vol. 8, no. 1, pp. 2–10, 2018.

[49]   X. Ma, Z. Yu et al. "How defects impact in vitro behavior of iron carboxylate MOF nanoparticles" Chem. Mater. 2023. Submitted

[50]   K. Guesh, C. Alves, *et al.*, "Sustainable preparation of MIL-100(Fe) and its photocatalytic behavior in the degradation of methyl orange in water," *Cryst. Growth Des.*, vol. 17, no. 4, pp. 1806–1813, 2017.

[51]   J. L. Zhuang, X. Y. Liu, *et al.*, "Hollow carbon polyhedra derived from room temperature synthesized iron-based metal-organic frameworks for supercapacitors," *J. Power Sources*, vol. 429, no. April, pp. 9–16, 2019.

[52]   K. L. Tan and K. Y. Foo, "Preparation of MIL-100 via a novel water-based heatless synthesis technique for the effective remediation of phenoxyacetic acid-based pesticide," *J. Environ. Chem. Eng.*, vol. 9, no. 1, p. 104923, 2021.

[53]   T. Steenhaut, S. Hermans, *et al.*, "Green synthesis of a large series of bimetallic MIL-100(Fe,M) MOFs," *New J. Chem.*, vol. 44, pp. 3847–3855, 2020.

[54]   H. Tian, J. Peng, *et al.*, "One-pot sustainable synthesis of magnetic MIL-100(Fe) with novel Fe3O4 morphology and its application in heterogeneous degradation," *Dalt. Trans.*, vol. 47, no. 10, pp. 3417–3424, 2018.

[55]   H. Reinsch, B. Bueken, *et al.*, "Green synthesis of zirconium-MOFs," *CrystEngComm*, vol. 17, no. 22, pp. 4070–4074, 2015.

[56]   R. Nivetha, K. Gothandapani, *et al.*, "Highly Porous MIL-100(Fe) for the Hydrogen Evolution Reaction (HER) in Acidic and Basic Media," *ACS Omega*, vol. 5, no. 30, pp. 18941–18949, 2020.

[57]   M. S. Peters and Klaus D. Timmerhaus, *Plant Design and Economics for Chemical Engineers*, 5th ed. Elizabeth A.Jones, 2003.

[58]   "Raw materials price - (a) https://www.icis.com/explore/resources/news/2005/12/02/517817/chemical-profile-ferrous-sulfate/(b) https://www.chemicalbook.com/Price/Trimesic-acid.html; (c) https://www.echemi.com/productsInformation/pd20150901041-caustic-soda-p." [Online]. Available: https://www.chemicalbook.com/Price/Trimesic-acid.html; [Accessed: 07-Jul-2021].

[59]   A. Rajendran, "Twitter post - Svante solutions announceshe use of CALF-20, a #MOF developed by G. Shimizu (@UCalgary), in its CO2 capture unit. Is this the first commercial large-scale applcn of a #MOF, esp. for #CCS? Productivity:30t CO2 cap/t MOF/day. Cost of MOF=$ 20," 2020. [Online]. Available: https://twitter.com/RajendranArvind/status/1334950716964630528.